PROCEEDINGS, 49th Workshop on Geothermal Reservoir Engineering
Stanford University, Stanford, California, February 12-14, 2024
SGP-TR-227

A Stochastic Optimization Model for a Ground Source Heat Pump System with Uncertainty Quantifications on Transient Geologic Variables

Zilong Zhao, Guoquan Lv, Yanwen Xu, Yu-Feng Lin, Pingfeng Wang and Xinlei Wang

Department of Agricultural and Biological Engineering, 1304 W. Pennsylvania Ave., University of Illinois at Urbana-Champaign, Urbana, IL 61801, USA

xwang2@illinois.edu

Keywords: ground source heat pump, geological factors, uncertainties, probabilistic modeling, cost minimization.

ABSTRACT

In this study, a stochastic model for optimizing the design configurations of a ground source heat pump (GSHP) with the objective of cost minimization was developed. Firstly, the concept of reliability-based design optimization (RBDO) is introduced by demonstrating the simulation workflow including linearization of workspace, steps of design optimization, and formulated constraints that are applied as reliability criteria to ensure a turbulent flow within the ground heat exchanger and avoid extreme temperature variations over seasonal operation. Furthermore, to enhance the model's fidelity, uncertainties pertaining to the groundwater velocity and ground thermal conductivity were incorporated as random variables in the optimization process. The stochastic characteristics of groundwater velocity are particularly investigated by using its temporal value profiles, considering both amplitude at specific time instances and transient variations over time. The utilization of normal distributions effectively addressed these characteristics. The efficacy of this novel model was demonstrated in yielding the minimized total costs during a GSHP's lifespan by concurrently addressing the uncertainties of the both design variables and geological parameters, ultimately reaching a state of convergence. The findings revealed that uncertainties related to geological factors can exert a significant influence on both the initial and operational costs of GSHP system. The optimized design variables, including borehole length, ground pipe radius, and working fluid flow rate, were provided at a confidence level of 85% across multiple predicted scenarios, ensuring the robustness and reliability of the GSHP system design.

1. INTRODUCTION

Ground source heat pump (GSHP) transfers the excessive heat and cold from building facilities to the subsurface body depending on the air conditioning requirements in different seasons. One of the most privileged advantages of GSHP system is its high efficiency compared not only to the traditional heating approaches such as furnace and district vapor heating, but also to the air source heat pump system, due to the stable temperature beyond 5 m-depth beneath the ground surface (Mao et al., 2023). On the other hand, to guarantee the effective heat transfer within the subsurface, boreholes need to be drilled to the proper length and arranged in clusters. This inevitably increases the initial cost for a GSHP system (Blum et al., 2011; Liu et al., 2019). It is recorded that the cost of drilling and ground heat exchanger (GHE) installations may account for over 50% of the system capital cost (Lu and Narsilio, 2019). For a typical vertical borehole, the length of borehole varies from 50 ~ 150 m depending on the capacity demand, civil land planning, and one often neglected factor—the geological conditions (Zhao et al., 2023; Sarbu and Sebarchievici, 2014). In brief, the majority of the studies conducted over the last decade were to reduce the upfront cost of GSHP by primarily introducing novel optimization scheme for the borehole design. Chang et al. (2023) found that integrating a PV-thermal curtain wall with a hybrid GSHP system improved its performance, enhancing the heat pump's COP by 5% and reducing life cycle costs and energy consumption. Ahmed et al. (2023) reviewed the growing use of machine learning for optimizing sustainable borehole heat pump systems, noting a threefold increase in studies over the last decade. Wang et al. (2022) demonstrated significant operational cost reductions and lower carbon emissions in a hotel's GSHP system by varying operational modes. Xie et al. (2020) employed a genetic algorithm to optimize a combined GSHP and radiant ceiling air conditioning system. Zhao et al. (2023) explored the benefits of implementing GSHP system into a LEED-certified green building.

However, most documented studies are focused on the deterministic design without taking the uncertainties, especially the probabilistic uncertainties, in the GSHP system into account. The concept of reliability-based design (Zhao et al., 2021), particularly regarding uncertainties in key variables, has been rarely explored in the field of GSHP. As a well-established mathematical tool, Reliability-based design optimization (RBDO) is widely adopted in the engineering practices, which aims to balance objectives such as cost and efficiency with reliability (Xu et al., 2023; Faes and Valdebenito, 2020). It involves using probabilistic indices and constraint functions to prevent suboptimal designs due to variable deviations. For example, in GSHP systems, variables including borehole length and water pump function significantly affect system performance. Typical RBDO models use mean values and deviation ranges to define such key variables, creating unique indices for them to ensure a local optimization while considering all uncertainty factors. Furthermore, the existing studies have revealed that the heterogeneity of the geology and the groundwater seepage may alter the thermal environment around the borehole and introduce significant impacts to the efficiency of GSHPs (Zhao et al., 2022; Luo et al., 2016). It was also found in studies that variables including groundwater seepage rate and water table may fluctuate over years (Chen et al., 2020; Bina et al., 2023). It is thus crucial to integrate the influence of dynamically varying geological factors into the optimization, which serves as the

other goal of this study. The contributions of this work are summarized as: a) a new robust RBDO model was proposed and tested to validate the feasibility of combining the reliability model and the stochastic profiles of environmental variables. Convergence maps were provided to show the model robustness under various GSHP operational conditions; and b) the optimization algorithm considers the transient characteristics of geological properties, mainly referring to the groundwater velocity. The independent and coupling impacts of the geological variables on the accumulative costs of a GSHP system were assessed. This holistic approach refines the original reliability-based design and provides deeper insights into system performance.

2. METHOD AND MODEL CONFIGURATIONS

2.1 The Simulation Procedures for RBDO

The workflow for the RBDO algorithm can be demonstrated using Figure 1. In this study, the objective of the simulation is set to minimize the total cost of the GSHP system over its 20-year lifespan. The depth of the borehole, the radius of the pipe, and the mass flow rate of the ground loop fluid are used as the design variables because the selection of them may significantly influence the performance of the GSHP system and thus they be modified during the design process. The geological parameters, such as the ground thermal conductivity and the groundwater velocity, are treated as random variables. This is because they are beyond designers' control and subject to change over time. The mathematical model utilizes the G-function as the fundamental iterative approach to calculate the accumulated temperature near the borehole area and compute the temperature profile of the working fluid in the U-pipe. Ultimately, it delivers the total cost for the GSHP system combining its capital cost and operational cost. As all optimization approached require, constraint functions are necessary when it comes to finding the local or global optimal point. In this study, three constraint functions were established for the working fluid in the U-pipe to regulate the optimizing direction of design variables—the turbulence state of the flow, the minimum pressure drop, and the minimum temperature at the end of the 20-year simulation. These constraints are commonly encountered in a GSHP study to ensure the heat transfer effectiveness in the GHE and avoid overcooling in the long term. The details of the calculation process can be found in Samson's model (Samson et al., 2018) and the setup of constraints can be accessed in our earlier work (Zhao, 2023).

Note that "f" in Figure 1 denotes the objective cost function, which is dependent on both design variables D (borehole depth, pipe radius, flow rate of working fluid) and random site variables X (ground thermal conductivity, groundwater velocity, and their increasing rates). ξ_j symbolizes the performance function for the j^{th} constraint. The vector d contains (d_1, ..., d_N), where $\mu(D)$ represents the mean values of the design variables. The terms d_i^L and d_i^U define the lower and upper bounds of the i^{th} design variable, d_i, respectively. R represents the system's reliability. Additionally, R^t stands for the targeted reliability level which is user-established for optimization. It is also equivalent to the target reliability index β^t, which can then be assessed using First-Order Reliability Method (FORM) (Hasofer and Lind, 1974). In FORM, the first step is to transform the design and random variables from the standard uniform domains to the standard normal domain U-space, which is based on the normal probability distribution. The core concept of FORM is to operate in U-space and linearize the constraint functions $\xi_i(U_i)$ at the point of highest likelihood of failure, known as the Most Probable Point (MPP), within the boundary of the limit state constraint equations. The MPP, located in the U-space, is the point on the failure boundary closest to the origin, representing the point of lowest reliability in the design. This closest distance is termed the reliability index (β^i). Consequently, the reliability of the system, R^i, is calculated using R^i = function(β^i) for each constraint. Following this, a sensitivity analysis is required to determine the rate of change of β^i in relation to each design variable. The performance measurement approach (PMA) (Zhao et al., 2021) was applied in the design optimization process and yield the new sets of values for design variables at each iteration. By updating the design variable and repeating the above-mentioned process, the optimal design (D*) can be ultimately obtained at the 85%-confidence reliability level.

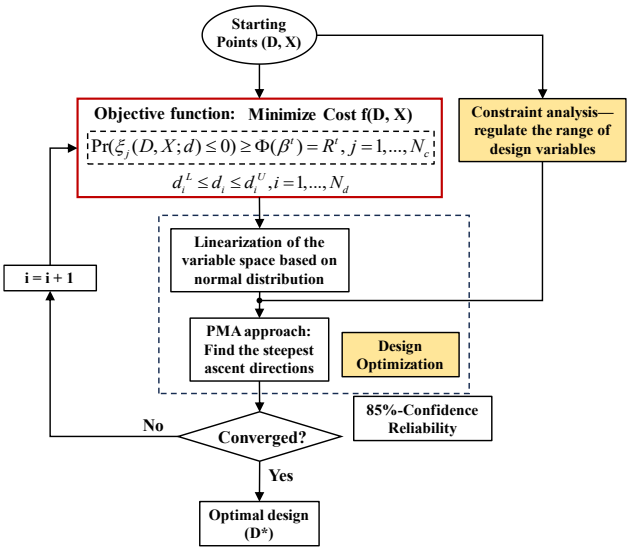

Figure 1: The RBDO workflow diagram.

2.2 The Applied Parameters in the Simulation Process

As introduced earlier, this study integrates the probabilistic profiles into the optimization. Therefore, the probabilistic indices for design and random variable are presented in Table 1. The established mean values and standard deviations (STDs) indicate how the values of variables may randomly fluctuate during the simulation. For instance, if the mean value of borehole depth (H) is set to be 80 m with a STD of 5 m, it implies a 68.3% probability that H will be within 75 ~ 85 m, and a 95.5% chance it will be within 70–90 m. In our previous work (Zhao et al., 2021), to accurately represent the uncertainties behind the design variables, relevant engineering brochures and literature were investigated and implemented in a comprehensive modeling work. Typically, the STDs for pipe radius and mass flow rate of the ground loop fluid can be maintained at 1 mm and 0.01 kg/s, respectively, which is based on findings summarized in (Bai and Bai, 2005), which relate to the accumulated roundness over the lifespan of pipelines. The STD of flow rate can be chosen in accordance with flow rate tests from the Ground Heat Exchanger (GHX) design manual (Geothermal Design Studio, 2016). Regarding STDs of ground thermal conductivity and groundwater velocity, respectively, insights and results from studies on geological uncertainty (Zhai and Benson, 2006; Lin et al., 2014) have demonstrated that the random variation of the former follows a normal distribution and the latter a log-normal distribution. However, in this study, to preliminarily investigate the transient groundwater velocity, the emphasis is given to the U_{rate} under the conditions with varied ground thermal conductivity. Therefore, it can be observed from the table that the STDs for all design variables were given with conservative magnitudes to show the independent effects of groundwater and improve the convergence of this simulation.

Table 1: Model Configurations in the RBDO Algorithm.

Design (D) & Random (X) Variables	Initial Values	Mean Values	Standard Deviations (STDs)	Units
D_1: Depth of the Boreholes	80	(30, 150)	1×10^{-4}	m
D_2: Pipe Radius	0.025	(0.01, 0.0375)	1×10^{-5}	m
D_3: Mass Flow Rate of Water	0.1	(0, 1)	1×10^{-4}	kg/s
X_1: Groundwater Velocity	5	5	0, 0.25	10^{-6} m/s
X_2: Ground Thermal Conductivity (K)	2	1 ~ 4 with a 0.5 interval	1×10^{-4}	W/m-K
X_3: Increasing Rate of Groundwater Velocity U_{rate}	0 ~ 0.4 with a 0.005 interval. STD = 0			-

3. SIMULATION RESULTS

3.1 Convergence of the Simulated Scenarios

Figure 2-4 illustrate the iterative plots of the residuals for the three specified constraints under four distinct scenarios based on varied U_{rate} and ground thermal conductivities (K). As presented in Table 2, the U_{rate} for these scenarios is set at 0, 0.5%, 2.5%, and 4%, and K at 2.0, 3.5, 4.0, and 2.5, respectively.

Table 2: Parameter Settings in the Four Scenarios.

Parameters	Scenario A	Scenario B	Scenario C	Scenario D
U_{rate}	0.5%	2.5%	3.5%	0
Ground thermal conductivity [W/(mK)]	2.0	3.5	4.0	2.5

The red dashed line in the first plot symbolizes the reliability target for the optimization, indicating that a locally optimized point is achieved only when all three constraints converge below this line, approaching zero. It is noticeable that, regardless of the changes in groundwater velocity, convergence is attainable in each scenario. As introduced earlier, the first constraint is to ensure the turbulence status of the flow. Therefore, the constraint function is set to be the difference between the simulated Reynolds number and the turbulent threshold 2300. One can observe that the trends of all four scenarios are likewise, the solver initially is seeking for a low pipe flow rate to reduce the operational electricity consumption, however, as the optimization process undergoes, the best balance between the potential cost and improved heat transfer efficiency is reached. When it comes to the convergence, all scenarios reached a relatively higher Reynolds number that satisfy the constraint. In contrast, the second and third constraints on pressure drop and fluid temperature

exhibit much smaller magnitude when compared to Reynolds number. Thus, the yielded residuals for them are observed in smaller magnitudes and approximating zero, the reliability safe line, which also indicates the solver has found a local optimal point under regulations. Additionally, the optimized accumulative costs for these scenarios are $66912, $60994, $58849, $69502, respectively. Notably, the highest cost occurs in the fourth scenario, characterized by no increase in groundwater velocity over time. This can be explained by the fact that when the groundwater seepage velocity is milder, it is likely to mitigate the convective heat transfer and the design would tend to be more conservative.

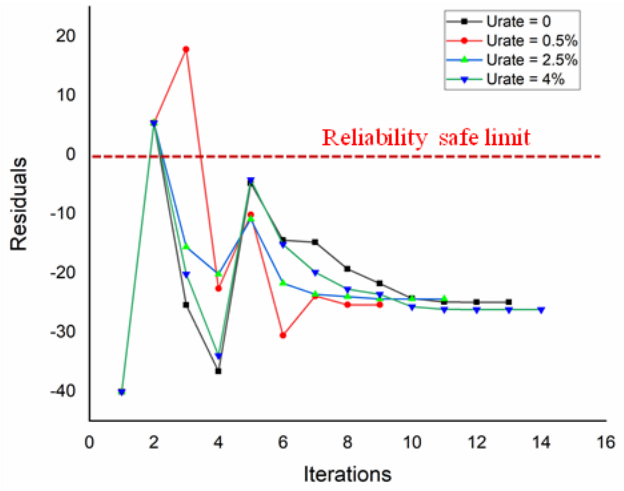

Figure 2: Residuals' plots of three constraint functions towards the increase of iterations for different simulated scenarios.

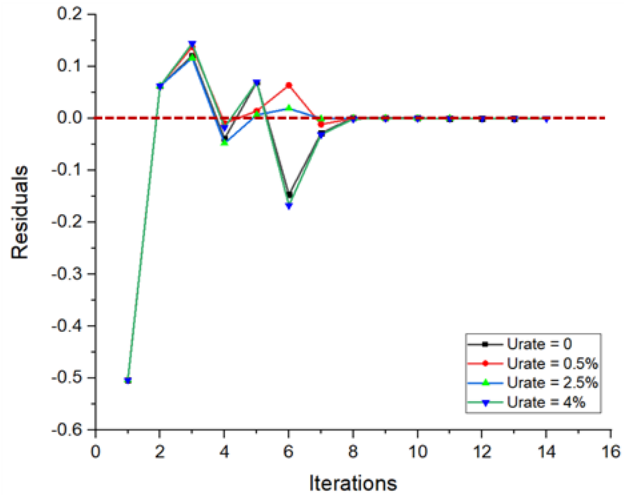

Figure 3: Residuals' plots of three constraint functions towards the increase of iterations for different simulated scenarios.

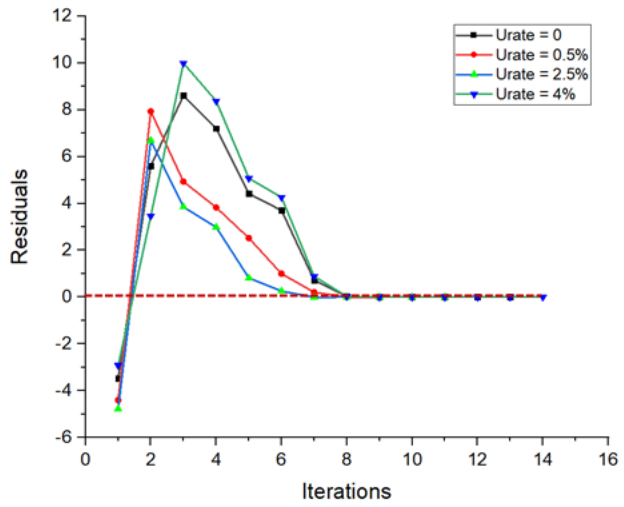

Figure 4: Residuals' plots of three constraint functions towards the increase of iterations for different simulated scenarios.

3.2 Impacts of the Increase and Standard Deviation of Groundwater Velocity

To more comprehensively explore the coupled effects of U_{rate} and K, the selected U_{rate} values were finely segmented with 0.5% increments within a 0 to 4% range to capture critical inflection points effectively. Moreover, accounting for the spatial variability of ground thermal conductivity is essential due to its significant influence on heat transfer performance near the borehole. As a result, the thermal conductivity of the soil's solid phase was divided into seven categories, ranging from 1 to 4 W/(mK), covering various geology that may exhibit active or poor heat transfer characteristics. Notably, in this part of the study, the standard deviations (STDs) of all variables were omitted in the optimization process to clearly observe the individual impacts of U_{rate}. The key results of the simulation—the borehole depth and the accumulative costs of the GSHP system over its lifespan, are depicted in Figure 5 and 6.

Firstly, an increase in ground thermal conductivity (K) typically leads to a rise in both the optimized H and the accumulative cost. More specifically, under constant and high U_{rate} values, the optimized borehole depth consistently increases as thermal conductivity rises. Conversely, when U_{rate} is below 1%, the optimized H initially increases and then decreases with increasing thermal conductivity. This is attributed to the dual effects of high thermal conductivity near the borehole area. On one side, it can enhance the GHE's heat transfer efficiency, potentially reducing the required borehole length. However, in geological settings with active aquifers where groundwater convection is dominant, rapid heat exchange near the borehole can cause significant thermal imbalances, necessitating a deeper borehole for even energy distribution. This balancing act is illustrated by a parabolic curve, where the largest borehole depth and cost occur near a thermal conductivity of 2 W/(mK). As expected, a higher groundwater velocity markedly decreases the optimized depth of boreholes. And when it comes to extremely high groundwater velocity, the solver optimized the borehole depths to be exactly on the lower limit, 30 meters. As it is highlighted in the graph, when U_{rate} is approximating 4% and K is near the lower limit, the depth of borehole tends to be reduced significantly. When U_{rate} remains as 4% and K increases from 2.5 to 4.0 W/(mK), the optimal depth of borehole increases from 30.7 to 40.4 m, with a 31.9% rise, to guarantee the thermal balance in the ground over long term and avoid overcooling.

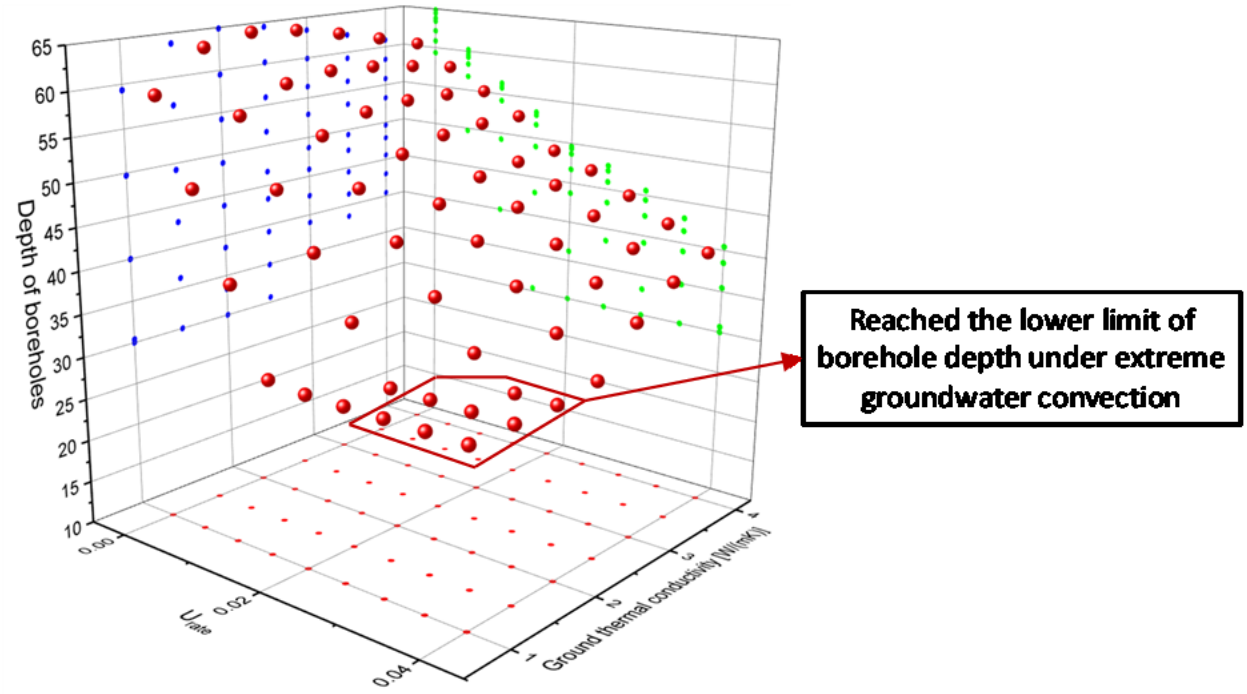

Figure 5: Mapping the optimal borehole depths considering variable rates of groundwater flow velocity and ground thermal conductivities.

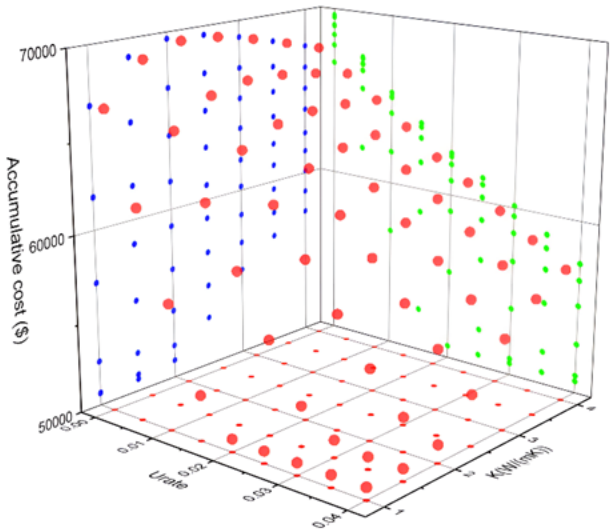

Figure 6: Mapping the minimized accumulative costs considering variable rates of groundwater flow velocity and ground thermal conductivities.

Furthermore, the optimal pipe radius for the ground loop in GHE and the internal flow rate are presented by Figure 7. It is noticeable that both parameters tend to be reduced when the groundwater velocity tends to increase faster, and the ground thermal conductivity is low. It indicates that as the groundwater convection magnifies and the heat conduction in the ground is dominated, the design may consider shrinking the size of the ground pipe and lower the flow rate to decrease the operational cost. In general, the values of mapped pipe radius fall within the range of 2 to 3 cm and under extreme conditions, the optimization outputs 3.14 cm, indicating the significantly higher heat conduction that can be obtained from the ground. In contrast, the flow rate primarily fall between 0.2 to 0.29 kg/s, and may exceed 0.293 kg/s when it comes to the right bottom corner in the graph.

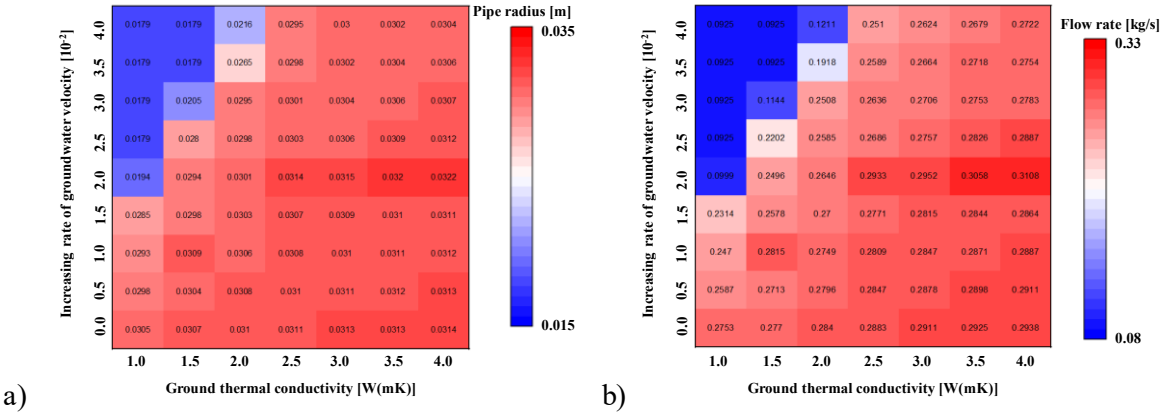

Figure 7: Mapping the a) optimal radius of the ground buried U-pipe and b) optimal flow rate of the working fluid in the U-pipe considering variable rates of groundwater flow velocity and ground thermal conductivities.

To preliminarily explore the probabilistic profile of groundwater flow, the comparison was also made between the case where the groundwater velocity is assigned with a mean value and a STD of 2.5×10^{-7} m/s (treatment) and the standard scenario (control) without considering either STD or U_{rate}. The difference in the results of the design variables and costs are presented by Figure 8. It can be observed that the difference of borehole depth and cost largely depends on the magnitude of the ground thermal conductivity (K). When K is 2.0 W/(mK), the lowest value among the selections, the stochastic characteristic of groundwater flow may impose more risks in overcooling phenomena over GSHP's lifespan. Therefore, the boreholes tend to be deeper than the standard control case. However, when K increases, the benefits of potentially having a high groundwater velocity exhibit. And when K rises to be 4.0 W(mK), the boreholes in the standard cases become over 1.3 deeper than the treatment. In contrast, the pipe radius and flow rate tend to be increasing at all selected K values, indicating that by considering the STD of groundwater velocity, the pumping activities should be designed more aggressive to realize better thermal efficiency.

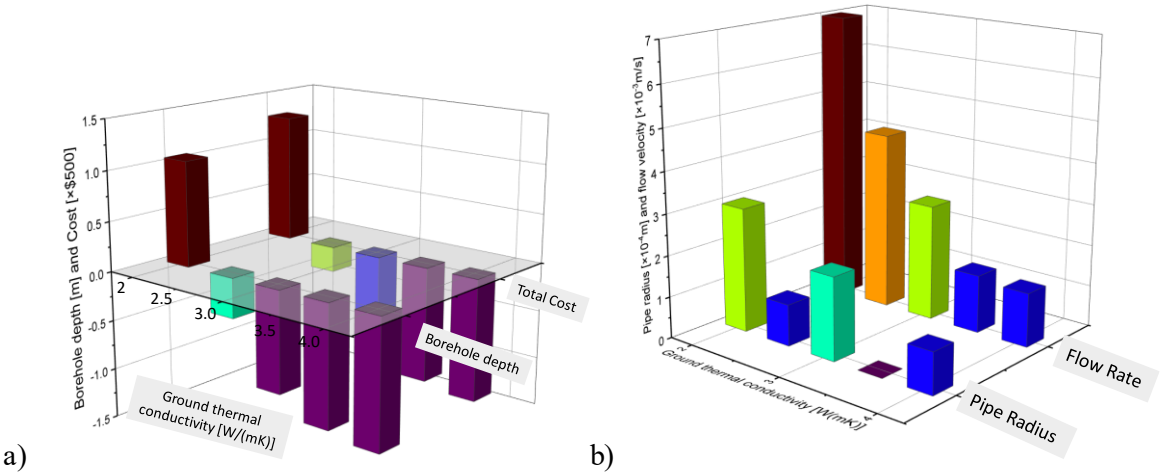

Figure 8: The difference between the optimized design variables and costs in scenario where the standard deviation of groundwater velocity at 2.5×10^{-7} m/s is applied and the standard scenario without considering it. The bars represent the difference between the two scenarios. For example, the borehole depth at around 1 m means that boreholes are 1 m deeper in the case considering STD of groundwater velocity.

4. CONCLUSIONS

This study applies reliability-based design optimization algorithm to a GSHP system with a simulated 20-year lifespan. The model integrates dynamic mean values of geological factors including groundwater velocity and ground thermal conductivity. Additionally, the stochastic standard deviation for the groundwater velocity was investigated. The uncertainties within the interested geological variables such as borehole depth, ground pipe radius, and pumping flow rate, based on their probability distributions, are also integrated into the model. The study focuses on how these factors affect the GSHP system's long-term cost-effectiveness by minimizing costs using iterative G-function analysis. All simulation cases achieved convergence, and the optimal combinations of borehole depth, pipe radius, and mass flow rate for the ground loop heat exchanger were obtained. Key findings include:

A) The integration of stochastic profiles of design and random variables in GSHP system into the cost minimization model has been proved to be feasible, as all simulated scenarios achieved convergence by satisfying the constraint functions.

B) Under the specified constraints where there is a lower limit for fluid temperature at the end of the simulation year, high groundwater velocity (about 5×10^{-6} m/s) may aid in decreasing the borehole depth because the groundwater seepage may refresh the thermal environment near the borehole and avoid overcooling.

C) Increases in ground thermal conductivity (K) would enhance the heat transfer rate between GHE and the geology. Without sufficient groundwater convection, this may result in deeper boreholes to ensure the even energy distribution and avoid thermal imbalance over long term. The depth of boreholes may experience 31.9% difference when K rises from 2.5 to 4.0 W/(mK).

D) When considering the probabilistic groundwater velocity, the impact of ground thermal conductivity (K) on borehole depth and cost is obvious. With the K value of 2.0 W/(mK), the stochastic nature of groundwater flow presents a higher risk of overcooling over the lifespan of the GSHP system. This leads to deeper boreholes compared to the standard control case. When K reaches 4.0 W(mK), the boreholes in standard scenario are over 1.3 m deeper than in the treatment case. On the other hand, both pipe radius and flow rate tend to increase across all selected K values in the treatment cases.

As the knowledge gaps are addressed by analyzing multiple uncertainty scenarios in this study, there are still limitations, however, needed to be highlighted for further research into more advanced GSHP systems. For instance, the hybrid GSHP systems combined with solar subsystems, the borehole thermal storage systems, etc. should be further investigated under stochastic optimization model such as RBDO to improve geothermal heat pump efficiency and economic competitiveness.

REFERENCES

Ahmed, N., Assadi, M., Ahmed, A. A., and Banihabib, R.: Optimal design, operational controls, and data-driven machine learning in sustainable borehole heat exchanger coupled heat pumps: Key implementation challenges and advancement opportunities, Energy for Sustainable Development, 74, (2023), 231–257.

Bai, Y. and Bai, Q.: Chapter 4 - Limit-state based Strength Design, Subsea Pipelines and Risers, (2005), 67-80.

Blum, P., Campillo, G., and Kölbel, T.: Techno-economic and spatial analysis of vertical ground source heat pump systems in Germany, Energy, 36, (2011), 3002-3011.

Bina, S. M., Fujii, H., Kosukegawa, H., and Katsuragi, M.: Evaluation of groundwater pumping impact on the thermal conductivity of neighboring ground source heat exchangers, Geothermics, 108, (2023), 102618.

Chang, S., Feng, G., Zhang, L., Huang, K., and Li, A.: Multi-objective optimization of a photovoltaic thermal curtain wall assisted dual-source heat pump system, Applied Thermal Engineering, 222, (2023), 119845.

Chen, N., Wen, H., Li, F., Hsu, S., Ke, C., Lin, Y., and Huang, C.: Investigation and Estimation of Groundwater Level Fluctuation Potential: A Case Study in the Pei-Kang River Basin and Chou-Shui River Basin of the Taiwan Mountainous Region, Applied Sciences, 12, (2022), 7060.

Faes, M. G. R. and Valdebenito, M. A.: Fully decoupled reliability-based design optimization of structural systems subject to uncertain loads, Computer Methods in Applied Mechanics and Engineering, 371, (2020), 113313.

Geothermal Design Studio. Ground Loop Design. 2016 Edition: Users' Manual. (2016).

Hasofer, A. M., Lind, N. S., Exact and Invariant Second-Moment Code Format, Journal of Engineering Mechanics, 100, (1974), 111-121.

Lin, W., Fulton, P. M., Harris, R. N., Tadai, O., Matsubayashi, O., Tanikawa, W., and Kinoshita, M.: Thermal conductivities, thermal diffusivities, and volumetric heat capacities of core samples obtained from the Japan Trench Fast Drilling Project (JFAST), Earth Planets Space, 66, (2014), 48.

Liu, X., Polsky, Y., Qian, D., and Mcdonald, J.: An Analysis on Cost Reduction Potential of Vertical Bore Ground Heat Exchangers Used for Ground Source Heat Pump Systems, Proceedings, 44th Workshop on Geothermal Reservoir Engineering, Stanford University, Stanford, CA (2019).

Lu, Q., and Narsilio, G. A.: Cost Effectiveness of Energy Piles in Residential Dwellings in Australia, Current Trends in Civil & Structural Engineering, (2019).

Luo, J., Rohn, J., Xiang, W., Bertermann, D., and Blum, P.: A review of ground investigations for ground source heat pump (GSHP) systems, Energy and Buildings, 117, (2016), 160-175.

Mao, R., Zhao, Z., Tian, L., Fang, T., and Wang, X.: Generation of Gridded Temperature Map of Constant-Temperature Layer Based on Meteorological Data for Shallow Geothermal Applications, Geothermics, 113, (2023), 102770.

Samson, M., Dallaire, J., and Gosselin, L.: Influence of groundwater flow on cost minimization of ground coupled heat pump systems, Geothermics, 73, (2018), 100-110.

Sarbu, L., and Sebarchievici, C.: General review of ground-source heat pump systems for heating and cooling of buildings, Energy and Building, 70, (2014), 441-454.

Wang, Y., Quan, Z., Zhao, Y., Wang, L., and Jing, H.: Operation mode performance and optimization of a novel coupled air and ground source heat pump system with energy storage: Case study of a hotel building, Renewable Energy, 201, (2022), 889-903.

Xie, Y., Hu, P., Zhu, N., Lei, F., Xing, L., and Xu, L.: Collaborative optimization of ground source heat pump-radiant ceiling air conditioning system based on response surface method and NSGA-II, Renewable Energy, 147, (2020), 249-264.

Xu, Y., Kohtz, S., Boakye, J., Gardoni, P., and Wang, P.: Physics-informed machine learning for reliability and systems safety applications: State of the art and challenges, Reliability Engineering & System Safety, 230, (2023), 108900.

Zhai, H. and Benson, C. H.: The Log-normal distribution for hydraulic conductivity of compacted clays: Two or three parameters? Geotechnical and Geological Engineering, 24, (2006), 1149-1162.

Zhao, Z., Lin, Y., Stumpf, A., and Wang, X.: Improving LEED-certified building loads on borehole heat exchangers by coupling subsurface variables, Applied Thermal Engineering, 224, (2023), 120119.

Zhao, Z., Lin, Y., Stumpf, A., and Wang, X.: Assessing impacts of groundwater on geothermal heat exchangers: A review of methodology and modeling, Renewable Energy, 190, (2022), 121-147.

Zhao, Z.: Assessing the impacts of geological factors on the Thermo-economic performance of Ground Coupled Heat Pump Systems. Assessing the impacts of geological factors on the thermo-economic performance of ground coupled heat pump systems | IDEALS. (2023).

Zhao, Z., Stumpf, A., Lin, Y., and Wang, X.: Impacts of prospective LEED building's energy loads on a borehole heat exchanger: A case study in Central Illinois, Proceedings of the IGSHPA Research Track, (2022).

Zhao, Z., Xu, Y., Lin, Y., Wang, X., and Wang, P.: Probabilistic modeling and reliability-based design optimization of a ground source heat pump system, Applied Thermal Engineering, 197, (2021), 117341.